

# Transverse Magnetic Anisotropy in Mn<sub>12</sub>-acetate: Direct Determination by Inelastic Neutron Scattering

Roland Bircher, Grégory Chaboussant, Andreas Sieber, and Hans U. Güdel

*Department of Chemistry and Biochemistry, University of Berne, Freiestrasse 3, CH-3000 Berne 9, Switzerland*

Hannu Mutka

*Institut Laue-Langevin, rue Jules Horowitz 6, BP 156, 38042 Grenoble Cedex 9, France*

(Dated: March 22, 2022)

A high resolution inelastic neutron scattering (INS) study of fully deuterated Mn<sub>12</sub>-acetate provides the most accurate spin Hamiltonian parameters for this prototype single molecule magnet so far. The Mn<sub>12</sub>-clusters deviate from axial symmetry, a non-zero rhombic term in the model Hamiltonian leading to excellent agreement with observed positions and intensities of the INS peaks. The following parameter set provides the best agreement with the experimental data:  $D = -0.0570(1)$  meV,  $B_4^0 = -2.78(7) \cdot 10^{-6}$  meV,  $B_4^4 = -3.2(6) \cdot 10^{-6}$  meV and  $|E| = 6.8(15) \cdot 10^{-4}$  meV. Crystal dislocations are not the likely cause of the symmetry lowering. Rather, this study lends strong support to a recently proposed model, which is based on the presence of several molecular isomers with distinct spin Hamiltonian parameters.

PACS numbers: 75.50.Xx, 75.45.+j, 75.30.Gw, 78.70.Nx

Single Molecule Magnets (SMM) are crystalline compounds consisting of nominally identical polynuclear molecular complexes of transition metal ions. They exhibit slow magnetisation relaxation phenomena at cryogenic temperatures. Discrete steps in the magnetisation are a typical feature directly related to quantum tunneling processes of the magnetisation (QTM). Mn<sub>12</sub>-acetate, [Mn<sub>12</sub>O<sub>12</sub>(OAc)<sub>16</sub>(H<sub>2</sub>O)<sub>4</sub>] $\cdot$ 2HOAc $\cdot$ 4H<sub>2</sub>O, was the first reported SMM and remains the best studied up till now. Since the pioneering work of Sessoli *et al.* [1, 2] Mn<sub>12</sub>-acetate has been extensively studied by INS [3, 4], EPR [5, 6], NMR [7], Raman and Infrared spectroscopy [8], specific heat [9, 10], micro-Hall probe techniques, micro-Squid techniques [11, 12, 13], magnetization relaxation [1, 9, 14, 15] and numerous other bulk measurements. Identifying and quantifying the interactions leading to slow relaxation and QTM has been the focus of several studies in very recent years [16, 17, 18, 19]. In this Letter we report a high resolution inelastic neutron scattering (INS) study on fully deuterated Mn<sub>12</sub>-acetate. In contrast to most other studies no external magnetic field is involved. This leads to very accurate values of the relevant interaction parameters responsible for QTM and allows us to unambiguously discriminate between the various microscopic models which have been proposed to account for the observed macroscopic behavior [16, 17].

[Mn<sub>12</sub>O<sub>12</sub>(OAc)<sub>16</sub>(H<sub>2</sub>O)<sub>4</sub>] $\cdot$ 2HOAc $\cdot$ 4H<sub>2</sub>O crystallizes in space group I $\bar{4}$ , and the [Mn<sub>12</sub>O<sub>12</sub>(OAc)<sub>16</sub>(H<sub>2</sub>O)<sub>4</sub>] molecule occupies a position with S<sub>4</sub> point symmetry [20]. The 4 H<sub>2</sub>O and 2 HOAc (acetic acid) solvent molecules are incorporated between the Mn<sub>12</sub>-acetate complexes, with the 2 HOAc disordered on a fourfold position. Exchange coupling between the Mn<sup>3+</sup> and Mn<sup>4+</sup> ions within the complexes leads to a  $S = 10$  ground state. A strong axial anisotropy with the S<sub>4</sub> axis as the easy axis

splits the ground state into sublevels from  $M_S = \pm 10$  to  $M_S = 0$  and thus creates the energy barrier which is responsible for the slow magnetisation relaxation phenomena at cryogenic temperatures. The appropriate spin Hamiltonian to account for this zero field splitting in the S<sub>4</sub> point group is given by [21]:

$$\hat{H}_{axial} = D \left[ \hat{S}_z^2 - \frac{1}{3} S(S+1) \right] + B_4^0 \hat{O}_4^0 + B_4^4 \hat{O}_4^4 \quad (1)$$

where  $\hat{O}_4^0 = 35\hat{S}_z^4 - [30S(S+1) - 25]\hat{S}_z^2 - 6S(S+1) + 3S^2(S+1)^2$  and  $\hat{O}_4^4 = \frac{1}{2}(\hat{S}_+^4 + \hat{S}_-^4)$ .

The first term of Eq. (1) is the leading term. Numerous parameter sets have been proposed, with those based on EPR and INS studies, which are very similar, usually considered the most reliable [3, 5]. Eq. (1) cannot account for all the observed QTM phenomena, in particular tunneling through  $M_S = \pm 10$  in zero field below 2 K. Additional terms to the ones in Eq. (1) are therefore needed. A Hamiltonian including a rhombic term of the form

$$\hat{H}_{aniso} = \hat{H}_{axial} + E(\hat{S}_x^2 - \hat{S}_y^2) \quad (2)$$

requires a deviation from the crystallographically determined S<sub>4</sub> molecular symmetry. This can result from the disorder in the solvent structure, and this possibility was examined in detail in Refs [17, 22]. The presence of six different geometrical molecular isomers with slightly different environments and thus different  $D$  and  $E$  parameters was postulated. An alternative model, in which the fourfold molecular symmetry is broken by crystal dislocations was proposed in Ref. [16]. This model corresponds to a broad distribution of site geometries with  $E$  values broadly distributed around  $|E| = 0$ . Very recent EPR and QTM studies strongly favor a discrete distribution

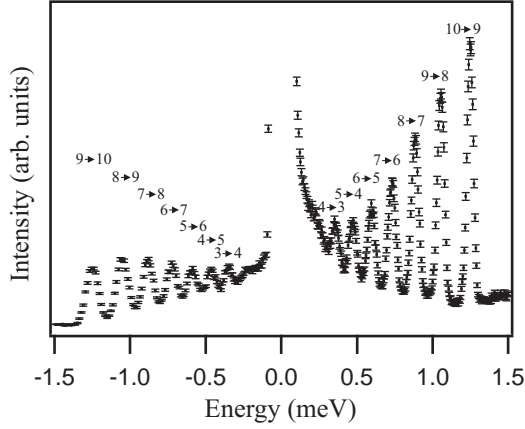


FIG. 1: INS spectrum measured on IN5 with an incident wavelength of  $\lambda = 5.9$  Å at 24 K for 15 h, summed over all scattering angles. The peaks are assigned to  $\Delta M_S = \pm 1$  transitions, see Figure 3a.

[18, 19], but exact parameter values to test the specific predictions of Refs [17, 22] are still missing.

In an earlier INS study of partially deuterated  $\text{Mn}_{12}$ -acetate the data were of sufficient quality to determine the three parameters  $D$ ,  $B_4^0$  and  $B_4^4$  in Eq. (1) [3]. The important question of an  $E$  term remained open. By an upgrade, the time-of-flight instrument IN5 at the ILL in Grenoble has gained an order of magnitude in speed, and data of significantly higher quality than in Ref. [3] are obtained. They allow a deeper analysis in terms of Eq. (2) and lead to a clear distinction between the proposed models. 6.5 g of a fully deuterated sample of  $\text{Mn}_{12}$ -acetate were used in the present study. The material was prepared as described in Ref. [20] using deuterated precursors and solvents. A cylindrical aluminum container of 14 mm diameter and 55 mm length was used for the INS experiments. Data were corrected for the background and detector efficiency using standard procedures. Figure 1 shows an overview INS spectrum ( $\lambda = 5.9$  Å) for a temperature  $T = 24$  K, at which all the  $M_S$  levels of the zero field split  $S = 10$  ground state have some population. The well developed and almost regular pattern of inelastic peaks on both the energy loss and energy gain sides (positive and negative energy transfer, respectively) are assigned to  $\Delta M_S = \pm 1$  transitions between adjacent ground state levels. This assignment is straightforward [3], since only  $\Delta M_S = \pm 1$  transitions are allowed in an axially zero field split state, see Figure 3a. Their relative intensities are calculated using Ref. [23]. The higher-order  $B_4^4$  and  $E$  terms in Eqs. (1) and (2) will mix  $M_S$  functions, and this becomes relevant in the following. The inner part of the INS pattern was measured at the same temperature with increased experimental resolution ( $\lambda = 8$  Å, *fwhm* of the elastic line  $23$   $\mu\text{eV}$ ). The result, displayed in Figure 2a, shows a sharpening of both the

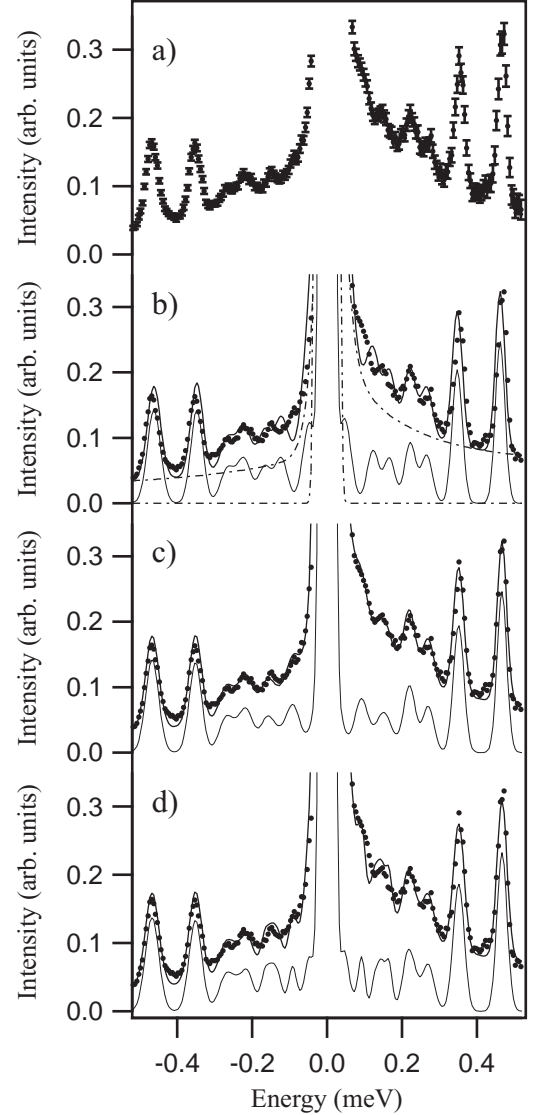


FIG. 2: a) INS spectrum measured with an incident wavelength of  $\lambda = 8$  Å at 24 K for 12.5 h, summed over all scattering angles. In b) to d) the same data are plotted without error bars including theoretical simulations. The same background, shown as dash-dotted lines in b), was used in all the calculations. b) Eq. (1),  $D$ ,  $B_4^0$  and  $B_4^4$  values in set I of Table I. c) Eq. (2), parameter set I in Table I. d) Eq. (2), parameter set III in Table I.

elastic and inelastic features and, in particular, some well resolved structure below 0.3 meV on both the gain and the loss side. In this spectral range the energy intervals and the relative intensities significantly deviate from the regular pattern observed in Figure 1. These deviations reflect the higher order terms in the spin Hamiltonian, and they will now be analysed. The data in Figure 2 are reproduced several times without error bars to allow comparisons with different theoretical models. The curve in Figure 2b corresponds to a calculation using Eq. (1)

			$D$ (meV)	$B_4^0$ ( $10^{-6}$ meV)	$B_4^4$ ( $10^{-6}$ meV)	$ E $ ( $10^{-4}$ meV)
I			-0.0570(1)	-2.78(7)	-3.2(6)	6.8(15)
II			-0.0570(1)	-2.78(7)	5.1(7)	5.3(9)
III	isomer	occupancy				
	0	0.0625	-0.0564	-2.78	-3.2	0
	4	0.0625	-0.0581	-2.78	-3.2	0
	1	0.25	-0.0564	-2.78	-3.2	6.9
	2cis	0.25	-0.0573	-2.78	-3.2	0.01
	2trans	0.125	-0.0573	-2.78	-3.2	13.8
	3	0.25	-0.0573	-2.78	-3.2	6.9

TABLE I: Parameter values obtained from fits to the experimental INS peak positions. I and II correspond to the minima in the goodness of fit plot in Figure 4. Set III corresponds to the model proposed in Ref. [17], but with  $D$  and  $|E|$  parameter values from Ref. [22]. The numbering of isomers is the same as in Refs [17, 22]. The  $B_4^0$  and  $B_4^4$  parameters are the same as in set I.

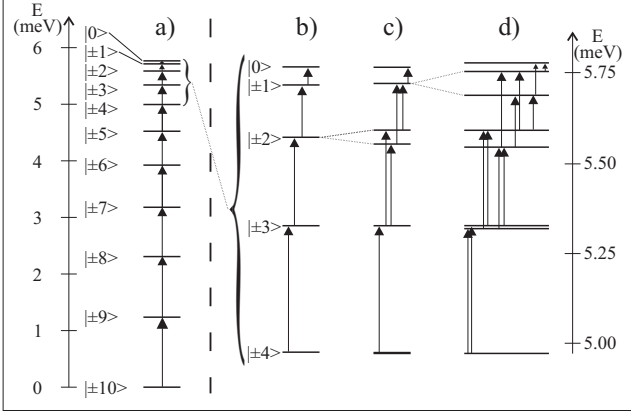


FIG. 3: Energy level splitting of the  $S = 10$  ground state and allowed (energy loss) INS transitions. a) Total splitting, purely axial. b) Upper part of a). c) Splitting of Eq. (1) and d) splitting of Eq. (2) with parameters in set I of Table I.

with the  $D$ ,  $B_4^0$  and  $B_4^4$  parameter values in set I of Table I. This is the best parameter set within the axial approximation, and it is the same within experimental error to the one derived previously using INS [3]. It is evident that for energy transfers below 0.3 meV there is poor agreement with the experimental data of the present study. The upper part of the energy splitting pattern for this calculation is shown in Figure 3c. The  $B_4^4$  term splits and mixes the  $M_S = \pm 2$  states in first order. Fitting our observed peak positions with the eigenvalues of Eq. (2), i.e. including an  $E$  term, leads to the calculated curve in Figure 2c. The best parameters are listed in set I of Table I. The calculated energy pattern is shown in Figure 3d. The  $E$  term splits and mixes the  $M_S = \pm 1$  states in first order, and this splitting is significant. This calculation shows a remarkably good agreement with the experiment, both in terms of peak positions and intensities. An almost equally good agreement is obtained with the parameter set II of Table I. The two solutions I and II correspond to negative and positive values of

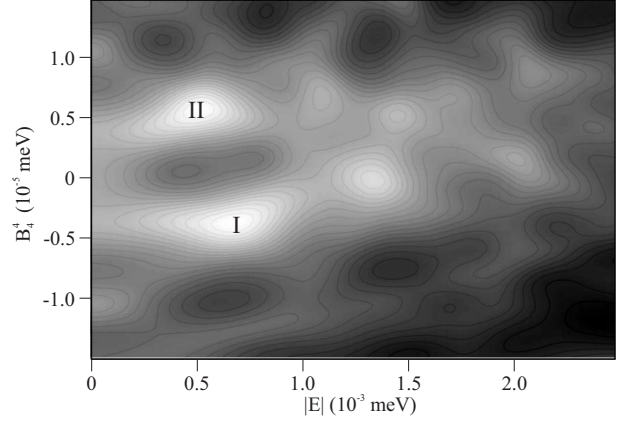


FIG. 4: Contour plot of the goodness of the fit of Eq. (2) to the experimental peak positions as a function of  $B_4^4$  and  $E$  with constant values for  $D$  and  $B_4^0$ . The two least-squares minima correspond to the parameter sets I and II in Table I.

the parameter  $B_4^4$ , respectively. In a purely axial model, eigenvalues for equal positive and negative  $B_4^4$  terms are degenerate. Figure 4 shows a contour plot, in which the goodness of the least-squares fit is plotted in the parameter space spanned by  $B_4^4$  and  $|E|$ . The two minima corresponding to the solutions I and II in Table I are very well defined. We confidently conclude that an  $E$  term is necessary to account for the observed INS data. And in contrast to earlier studies we can quantify the  $|E|$  parameter:  $|E| = 6.8(15) \cdot 10^{-4}$  meV and  $|E| = 5.3(9) \cdot 10^{-4}$  meV for solutions I and II, respectively. Of the two parameter sets we give preference to set I, i.e. a negative  $B_4^4$  parameter, because our value  $B_4^4 = -3.2(6) \cdot 10^{-6}$  meV lies close to the most recent and very accurate determination by EPR of  $|B_4^4| = 3.8(1) \cdot 10^{-6}$  [19].

Of the two models proposed in the literature to account for a deviation from axial molecular symmetry we definitely rule out the dislocation model [16], because it corresponds to a broad distribution of sites with  $E$  terms centered around  $|E| = 0$ . This is the energy level pat-

tern in Figure 3c and would lead to a broadened version of the calculated spectrum in Figure 2b. The alternative model with a set of six discrete sites for the  $\text{Mn}_{12}$ -acetate molecule [17] has recently received qualitative support from both EPR and tunneling studies [18, 19]. In Ref. [17] the  $D$  and  $E$  parameters of the six isomers were estimated on the basis of the angular overlap model. Based on the same isomer distribution model  $D$  and  $E$  parameters obtained by a density functional theory (DFT) calculation were recently reported [22]. The distribution of  $D$  and  $E$  values is very similar to Ref. [17], but the absolute values are more reliable. We calculated the energy splitting patterns for the six isomers and the corresponding INS spectrum at 24 K, using the  $D$  and  $|E|$  values from Ref. [22] and our best  $B_4^0$  and  $B_4^4$  values, see set III in Table I. The result is shown in Figure 2d. The agreement with the experimental data is remarkably good, considering that no adjustment of the  $D$  and  $|E|$  parameters was attempted. It is not *a priori* clear why the distribution of six species with populations and parameter values as given in set III of Table I gives a discrete INS spectrum with well defined peaks. Inspection of the parameter set III in Table I reveals that the three isomers 1, 2 cis and 3 make up 75% of all complexes in the crystal. The isomers 1 and 3 have very similar  $D$  and, more importantly in this context, practically identical  $|E|$  parameters to our best parameter set I. This, together with some near coincidences of transition energies for the other isomers, leads to a discrete spectrum which is in good agreement with experiment. Our study thus provides support for the model proposed in Ref. [17] and refined in Ref. [22].

Our spectroscopic study thus clearly reveals that the  $\text{Mn}_{12}$ -acetate clusters in  $[\text{Mn}_{12}\text{O}_{12}(\text{OAc})_{16}(\text{H}_2\text{O})_4]\cdot 2\text{HOAc}\cdot 4\text{H}_2\text{O}$  deviate from axial symmetry. A rhombic term in the spin Hamiltonian is essential, and all three parameter sets in Table I reproduce the INS spectra very well. Earlier studies based on Landau-Zener (LZ) magnetisation relaxation [18] and EPR [19] measurements provided upper limits of  $8.7 \cdot 10^{-4}$  meV and  $12.4 \cdot 10^{-4}$  meV, respectively, for the  $|E|$  values in the most strongly rhombically distorted complexes in  $\text{Mn}_{12}$ -acetate. Our study significantly narrows down the range of possible  $|E|$  values. In contrast to LZ and EPR measurements we are not primarily probing the complexes with the fastest relaxation or the strongest rhombic distortion but the total of all complexes. And the  $|E| = 6.8(15) \cdot 10^{-4}$  meV value of set I in Table I represents this. If we adopt the isomer distribution model, this value accounts for 50% of all the complexes; for 37.5% the  $|E|$  value is at least an order of magnitude smaller, and for 12.5% it is  $13.8 \cdot 10^{-4}$  meV. This latter value is in reasonable agreement with upper limit estimates of  $8.7 \cdot 10^{-4}$  meV and  $12.4 \cdot 10^{-4}$  meV from LZ and EPR, respectively. Interestingly, it was recently suggested, based on EPR experiments, that in deuterated  $\text{Mn}_{12}$ -acetate the upper limit of  $|E|$  was

$24.8 \cdot 10^{-4}$  meV, twice as high as for the undeuterated material [24]. This value is high and outside the range of our parameter values. Our experiment was performed on a completely deuterated sample, and we took great care to handle it in a water free atmosphere. In a sample which is not fully deuterated there is additional disorder in the acetic acid and water structure, and this could possibly lead to a broader distribution of rhombic distortions and thus  $|E|$  values. Rhombic distortions of individual complexes, likely caused by disorder in the solvent structure, are responsible for some of the observations in QTM measurements which are not compatible with a purely axial model. The present study provides quantitative information about the size of the rhombic parameters. This model is not able to account for the observation in  $\text{Mn}_{12}$ -acetate of QTM between levels with odd  $\Delta M$  values. Possible mechanisms have been proposed in Refs [16, 17, 25]. These effects must be small and our experiment provides no information to quantify them.

The authors acknowledge useful discussions with Oliver Waldmann. This work was supported by the Swiss National Science Foundation and the TMR programmes Molnanomag and Quemolna of the European Union (HPRN-CT-1999-00012 and MRTN-CT-2003-504880).

- 
- [1] R. Sessoli *et al*, Nature **365**, 141 (1993).
  - [2] R. Sessoli *et al*, J. Amer. Chem. Soc. **115**, 1804 (1993).
  - [3] I. Mirebeau *et al*, Phys. Rev. Lett. **83**, 628 (1999).
  - [4] Y. Zhong *et al*, J. App. Phys. **85**, 5636 (1999).
  - [5] A. L. Barra, D. Gatteschi and R. Sessoli, Phys. Rev. B **56**, 8192 (1997).
  - [6] S. Hill *et al*, Phys. Rev. Lett. **80**, 2453 (1998).
  - [7] Y. Furukawa *et al*, Phys. Rev. B **62**, 14246 (2000).
  - [8] A. B. Sushkov *et al*, Phys. Rev. B **63**, 214408 (2001).
  - [9] A. M. Gomes *et al*, Phys. Rev. B **57**, 5021 (1998).
  - [10] F. Luis *et al*, Phys. Rev. Lett. **85**, 4377 (2000).
  - [11] L. Thomas *et al*, Nature **383**, 145 (1996).
  - [12] B. Barbara *et al*, J. Phys. Soc. Jpn. **69**, Suppl. A., 383 (2000).
  - [13] I. Chiorescu *et al*, Phys. Rev. Lett. **85**, 4807 (2000).
  - [14] Y. Zhong *et al*, Phys. Rev. B **62**, 9256 (2000).
  - [15] L. Bokacheva, A. D. Kent and M. A. Walters, Phys. Rev. Lett. **85**, 4803 (2000).
  - [16] E. M. Chudnovsky and D. A. Garanin, Phys. Rev. Lett. **87**, 187203 (2001).
  - [17] A. Cornia *et al*, Phys. Rev. Lett. **89**, 257201 (2002).
  - [18] E. del Barco *et al*, Phys. Rev. Lett. **91**, 47203 (2003).
  - [19] S. Hill *et al*, Phys. Rev. Lett. **90**, 217204 (2003).
  - [20] T. Lis, Acta Crystallog. Sec. B **36**, 2042 (1980).
  - [21] D. Gatteschi and R. Sessoli, Angew. Chem. Int. Ed. **42**, 268 (2003).
  - [22] K. Park *et al*, Phys. Rev. B **69**, 144426 (2004).
  - [23] J. R. Birgenau, J. Phys. Chem. Solids, **33**, 59 (1972).
  - [24] E. del Barco *et al*, cond-mat/0404390 (unpublished).
  - [25] S. Hill *et al*, cond-mat/0401515 (unpublished).